HHS Public Access

Author manuscript

New Phytol. Author manuscript; available in PMC 2018 June 01.

Published in final edited form as:

New Phytol. 2017 June ; 214(4): 1673–1687. doi:10.1111/nph.14517.

Diverse mechanisms of resistance to *Pseudomonas syringae* in a thousand natural accessions of *Arabidopsis thaliana*

André C. Velásquez[#1], **Matthew Oney**[#1], **Bethany Huot**[1,2], **Shu Xu**[1,3], and **Sheng Yang He**[1,4,5,6]

[1]MSU-DOE Plant Research Laboratory, East Lansing, MI 48824, USA

[2]Cell and Molecular Biology Program, Michigan State University, East Lansing, MI 48824, USA

[3]Institute of Botany, Jiangsu Province and Chinese Academy of Sciences, Nanjing 210014, P. R. China

[4]Department of Plant Biology, Michigan State University, East Lansing, MI 48824, USA

[5]Plant Resilience Institute, Michigan State University, East Lansing, MI 48824, USA

[6]Howard Hughes Medical Institute, Gordon and Betty Moore Foundation, Michigan State University, East Lansing, MI 48824, USA

[#] These authors contributed equally to this work.

Keywords

Arabidopsis thaliana; AvrPto; effector-triggered immunity (ETI); plant pathogen; plant immunity; *Pseudomonas syringae* pv. *tomato* DC3000; resistance mechanisms; salicylic acid (SA)

Introduction

Genetic variation is crucial for the survival of all organisms and for crop improvement (Glaszmann *et al.*, 2010). It is in the untapped potential of uncharacterized individuals within a population where we may find new and improved traits for plant adaptation and resilience (Riely & Martin, 2001; Saintenac *et al.*, 2013). One of the major deterrents to crop productivity is disease. It is estimated that the actual loss of productivity due to pathogens for the major cultivated crops is close to 14% (Oerke, 2006). This loss of productivity could be reduced if the plant's defense mechanisms against pathogens could be heightened.

Plants have intricate defense mechanisms that impede pathogen colonization and infection, and that minimize fitness costs to the infected plants. Two defense mechanisms that occur

Author for correspondence: *Sheng Yang He, Tel: +1 517 353 9181, hes@msu.edu.*

Author contributions

A.C.V. designed and performed most of the experiments, analyzed the data, and wrote the manuscript; M.O. designed and performed the screen and the initial characterization of the accessions; B.H. performed experiments and analyzed the data, S.X. performed experiments; and S.Y.H. designed and supervised the experiments, and wrote the manuscript.

Supporting Information

Additional Supporting Information may be found online in the Supporting Information tab for this article:

almost in parallel when a plant encounters a potential pathogen are pathogen-associated molecular pattern (PAMP)-triggered immunity (PTI) and effector-triggered immunity (ETI) (Jones & Dangl, 2006). During PTI, epitopes of molecules ubiquitously present in microbes (*e.g.*, flagellin for bacteria and chitin for fungi) are perceived by pattern-recognition receptors (PRRs), which ultimately contributes to halted microbial growth (Zipfel *et al.*, 2004; Wan *et al.*, 2008). How this is achieved is not currently well defined. Successful pathogens are able to dampen PTI responses, mainly by the activity of toxins and effector proteins (Melotto *et al.*, 2006; Cheng *et al.*, 2011; Xiang *et al.*, 2011). However, certain plant individuals carry specific resistance (R) proteins that recognize either the presence or the activity of effectors, which ultimately triggers ETI (Grant *et al.*, 1995; Gassmann *et al.*, 1999). ETI usually leads to a localized programmed cell death response, the hypersensitive response, in the cells that are in contact with the pathogen, a phenomenon that is thought to limit pathogen spread. However, the boundaries distinguishing PTI and ETI are not as clear, as in nature both responses form a continuum (Thomma *et al.*, 2011).

Phytohormones influence both PTI and ETI (Tsuda *et al.*, 2009). Salicylic acid (SA) is a phenolic hormone involved in local defense as well as systemic acquired resistance (SAR), the latter of which protects infected plants from future pathogen colonization in uninfected tissue (Fu & Dong, 2013). Accumulation of SA increases after PTI elicitation (Tsuda *et al.*, 2008), and pre-treatment of plants with an SA analogue potentiates several flagellin responses (Tateda *et al.*, 2014). As for the involvement of salicylic acid in ETI, SA biosynthesis is partially required for effective ETI in some, but not all, effector-R protein pairs (Tsuda *et al.*, 2009). Furthermore, SA accumulation increases in a biphasic manner during ETI (Malamy *et al.*, 1990), while enzymatic depletion of SA accumulation causes ETI pathogen containment (but not cell death) to fail (Mur *et al.*, 1997).

Until now, studies on plant resistance have focused on a limited number of natural accessions or cultivars of a plant species. A fundamental question that remains to be answered in plant–pathogen interactions is how many types of resistance mechanisms a given plant species would already possess to defend against a potential pathogen that apparently has not co-evolved with the plant. *Pseudomonas syringae* pv. *tomato* (*Pst*) DC3000 is a phytobacterial pathogen that has been extensively studied for its ability to infect tomato (from which it was initially isolated; Cuppels, 1986) and Arabidopsis (Whalen *et al.*, 1991), and has been used as a model to probe plant defense responses (Xin & He, 2013). *Pst* DC3000 delivers more than 30 effector proteins into the plant cell using a type III secretion system (T3SS) (Wei *et al.*, 2015), which collectively with a phytotoxin, coronatine (Melotto *et al.*, 2006), are the two most important virulence-promoting mechanisms of this pathogen. Thus far, several studies have evaluated the variation in disease resistance to *P. syringae* in Arabidopsis, the largest of which examined 75 Arabidopsis accessions (Kover & Schaal, 2002; Perchepied *et al.*, 2006; Hossain & Sultana, 2015). To address the question of how many types of resistance mechanisms a given plant species would already possess to defend against a potential pathogen that has potentially not co-evolved with the plant, we investigated the responses of over 1,000 Arabidopsis accessions to infection by *Pst* DC3000 and identified 14 accessions that were resistant. Further characterization separated these accessions into four defined categories: (1) two accessions were only resistant if bacteria were inoculated onto the leaf surface; (2) six accessions were able to mount an ETI-like

response; (3) three accessions showed increased basal SA accumulation; and (4) three accessions did not fall into any of the previous three categories. AvrPto and HopAM1 were identified as effectors that influence the resistance in several accessions that show an ETI-like response to *Pst* DC3000. These results highlight the diverse mechanisms of resistance already in place in individuals of a population even before exposure to a particular pathogen strain occurs and, like in tomato, AvrPto recognition appears to play a prominent role in mediating the ETI-type interaction between *A. thaliana* and *Pst* DC3000.

Materials and Methods

Materials and methods detailing the crosses between Arabidopsis accessions, next-generation sequencing (NGS), SHOREmap mapping of resistance loci, and statistical analyses are described in the Supporting Information Methods S1–S3 and Notes S1.

Bacterial strains and antibiotics

Pseudomonas syringae van Hall strains were grown in modified LB (LM; 10 g l^{-1} tryptone, 6 g l^{-1} yeast extract, 1.5 g l^{-1} KH_2PO_4, 0.6 g NaCl, and 0.4 g $MgSO_4$•$7H_2O$) or King's B medium at 30°C, while *Escherichia coli* (Migula) Castellani and Chalmers strains were grown in LB (Lennox) medium at 37°C (Table S1). Antibiotics were used at the following concentrations: 100–400 μg ml^{-1} for ampicillin, 50 μg ml^{-1} for kanamycin, 100 μg ml^{-1} for rifampicin, and 50 μg ml^{-1} for spectinomycin.

Plant growth conditions

Arabidopsis thaliana (L.) Heynh seeds were stratified for 6 d at 4°C before sowing. Before stratification, seeds were incubated with 1.8% sodium hypochlorite for 15 min, since two accessions, Xan-2 and Xan-5, require this treatment for even germination. Plants were grown in a growth chamber with a 12-h photoperiod and a temperature of 23°C during the day and 21°C during the night, under a partially covered transparent dome.

Construction of Pst Δ*hopAM1-1*Δ*hopAM1-2* mutant

Pst DC3001 is a strain that has a *c.* 10-kb deletion in *Pst* DC3000 plasmid A that includes *hopAM1-2* (Landgraf *et al.*, 2006). Deletion of *hopAM1-2* in *Pst* DC3001 was confirmed using three primers; P1, P5, and T1 (Table S2); and GoTaq® DNA polymerase (Promega), as PCR would produce amplicons of different sizes for wild-type *Pst* DC3000 and mutated *Pst* DC3001. *Pst ΔhopAM1-1ΔhopAM1-2* mutant was constructed following a previously described procedure (Kvitko & Collmer, 2011). Effector *hopAM1-1* was deleted from *Pst* DC3001 by conjugation, integration of the deletion construct, and sucrose counter-selection of double crossover strains using *E. coli* S17-1 pCPP5914 (pK18mobsacB::*ΔhopAM1-1*; Cunnac *et al.*, 2011). After sucrose counter-selection, genomic DNA was extracted from several putative deletion strains using Gentra Puregene Yeast/Bact. kit (QIAGEN). Deletion of *hopAM1-1* from *Pst* DC3001 was confirmed using polymerase chain reaction (PCR) with primers P2615 and P2616 and Phusion® high-fidelity DNA polymerase (Thermo Fisher Scientific).

Plasmid transformation into *Pseudomonas syringae* followed the protocol of Choi *et al.* (2006). *Pseudomonas* cultures were grown until they reached an absorbance at 600 nm of 0.5–0.8, washed twice with 0.5 M sucrose, and then used to electroporate the corresponding plasmids using the following parameters: 1.8 kV, 25 μF, and 200 Ω.

Screen for *Arabidopsis thaliana* accessions resistant to *Pst* DC3000

Arabidopsis accessions used in the screen included an initial set of 96 accessions from a study that evaluated genetic polymorphism in *A. thaliana* (Nordborg *et al.*, 2005), and all the available accessions at the Arabidopsis Biological Resource Center (ABRC; The Ohio State University, USA) on February of 2009 (Table S3). Five-week-old plants were inoculated by dipping them into a *Pst* DC3000 suspension of 2×10^8 colony-forming units (CFU) ml^{-1} with 0.025% Silwet L-77. Plants were left covered under a transparent plastic dome for the duration of the experiment, in order to maintain high humidity. At 5 d post-inoculation, plants were evaluated for disease symptoms. Inoculated accessions lacking conspicuous disease symptoms (chlorosis, necrosis, or leaf collapse) were selected for further study.

Bacterial multiplication assays

Dip inoculation was done as described for the screen except that bacteria were resuspended in 0.25 mM $MgCl_2$ to an inoculum of 10^8 CFU ml^{-1}. For infiltration-based inoculation, leaves of 4–4.5-wk-old-Arabidopsis plants were poked with a needle and infiltrated with a bacterial suspension of 1×10^5 to 5×10^6 CFU ml^{-1} in 0.25 mM $MgCl_2$ using a needleless syringe. After the infiltrated leaves dried (*c.* 1 h post infiltration), plants were left covered under a transparent dome for the duration of the experiment. At least three plants were inoculated per treatment to evaluate bacterial multiplication.

To evaluate if the accessions exhibited accelerated cell death in response to high bacterial inoculum, leaves were infiltrated with a bacterial suspension of 10^8 CFU ml^{-1} in 0.25 mM $MgCl_2$ using a needleless syringe. After the infiltrated leaves dried, plants were left partially covered with a transparent dome for the duration of the experiment. Between 18–96 h post-inoculation, plants were evaluated for cell death. Individual leaves were visually categorized as having no necrosis, partial necrosis, or full cell death (Fig. S1). Alternatively, when individual effectors were expressed from *Pst Δ28E* strain, leaves were categorized as either showing no observable changes or chlorosis. At least four leaves from different plants were inoculated per treatment.

Hormone quantification

Hormones were extracted and quantified as described previously (Zeng *et al.* 2011). Approximately 50 mg of frozen leaf tissue was ground and then incubated at 4°C for 20 h in 80% methanol containing 0.1% formic acid, 0.1 g l^{-1} butylated hydroxytoluene (BHT), and 100 nM deuterated abscisic acid (ABA-d_6, courtesy of Dr A. Daniel Jones, as an internal standard to account for hormone loss during extraction). Samples were vortexed, centrifuged and filtered using 0.2-μm PTFE filter units (Merck KGaA), and the flow through was used for hormone quantification.

Ten µl of plant extracts were injected onto an Ascentis® Express C18 column (50 × 2.1 mm, 2.7 µm; SIGMA-Aldrich) installed in the column heater (50°C) of an Acquity Ultra Performance Liquid Chromatography (UPLC) system (Waters Corp.). For UPLC separation, we used a 5-min gradient method starting with a 9 : 1 mixture (v/v) of 0.1% aqueous formic acid (solvent A) and 100% methanol (solvent B) and increasing linearly to 100% solvent B with a mobile phase flow rate of 0.4 ml min^{-1}. After separation, samples were injected into a Quattro Premier XE mass spectrometer (Waters Corp.) equipped with an electrospray ionization (ESI) source operated in negative ion mode. Capillary voltage, cone voltage, and extractor voltage were set to 3.5 kV, 25 V, and 5 V, respectively, with the source temperature set to 120°C and the desolvation temperature set to 350°C. Desolvation gas and cone gas were set to flow rates of 600 l h^{-1} and 50 l h^{-1}, respectively.

Selected ion monitoring (SIM) was performed to quantify ABA (m/z 263.1>153.1), ABA-d_6 (m/z 269.1>159.1), jasmonic acid (JA; m/z 209.1>59), jasmonoyl isoleucine (JA-Ile; m/z 322.2>130.1), SA (m/z 137>93), and SA glucoside (SAG; m/z 299.1>137). The QuanOptimize software was used to identify the parent and daughter SIM pairs, and the QuanLynx software 4.1 (Waters Corp.) was used to determine analyte responses relative to the internal standard ABA-d_6. Hormones were quantified using standard curves prepared with purified hormones for each compound (hormones were purchased from SIGMA-Aldrich, except for JA-Ile, which was a kind gift from Dr Paul Staswick and SAG, for which the SA standard was used). Total SA was calculated by adding SA and SAG concentrations. Final concentrations are expressed as ng of hormone per gram of sample fresh weight (FW).

Benzothiadiazole (BTH) treatment

Arabidopsis accessions were sprayed with a solution of 0.025% Silwet L-77 with or without 100 µM BTH until the plants were thoroughly wet. Twenty-four hours after spraying, leaf tissue was collected and frozen for further analysis.

Protein extraction

Frozen leaf tissue was ground using the TissueLyser II homogenizer (QIAGEN) and 3-mm zirconium oxide beads (Glen Mills Inc.). Ground tissue was incubated for 10 min at 4°C with 3 volumes of extraction buffer (0.5% Triton X-100, 150 mM NaCl, 100 mM Tris-HCl pH 7.5, 10 mM dithiothreitol (DTT), 5 mM EDTA, and protease inhibitor cocktail for plant cell and tissue extracts; SIGMA-Aldrich) per mg of tissue to extract proteins. After removal of tissue debris, protein concentration was determined using the Bradford method (Bio-Rad protein assay), so that equivalent protein concentrations would be used for every sample.

Electrophoresis and Western blot

Polyacrylamide gel electrophoresis (PAGE) was performed using the NuPAGE® electrophoresis system (Thermo Fisher Scientific) and NuPAGE® Novex® 4–12% Bis-Tris gels. Proteins were transferred to polyvinylidene difluoride (PVDF) membranes and stained with Ponceau S stain (0.1% Ponceau S in 5% acetic acid) to confirm efficient transfer. Western blotting was done using α-PR1 (courtesy of Dr Xinnian Dong) and α-rabbit IgG-HRP (Thermo Scientific) antibodies. Protein detection used SuperSignal™ West Dura

extended duration substrate (Thermo Fisher Scientific) and Blue Ultra Autoradiography films (GeneMate).

Reactive oxygen species (ROS) detection

ROS production was detected using a luminol-based assay. Four-mm-diameter-leaf discs were placed on white 96-well plates (Greiner Bio-One International) and floated overnight in water. The next day, water was removed and leaf discs floated in a 2×10^8 CFU ml^{-1} *Pst* DC3000 suspension in 0.25 mM $MgCl_2$, 34 μg ml^{-1} of luminol (Sigma-Aldrich) and 10 μg ml^{-1} of horseradish peroxidase (type VI-A; Sigma-Aldrich). Luminescence was detected with a SpectraMax L microplate reader (Molecular Devices) using 1.5–2-s-integration intervals. Each treatment had 6–8 samples and each biological repeat was done in triplicate or quadruplicate.

Results

In order to discover as many types of *A. thaliana* resistance mechanisms to *Pst* DC3000 as possible, a large collection of 1,041 *A. thaliana* accessions obtained from the Arabidopsis Biological Resource Center (ABRC, The Ohio State University) (Table S3) were infected by dip-inoculation into a suspension of *Pst* DC3000. Fourteen accessions did not show any disease symptoms and were classified as being resistant to infection by *Pst* DC3000 (Fig. S2). Their geographic collection origin did not reveal any distinguishable pattern, as they were scattered throughout the native range of *A. thaliana*, which is restricted to Europe, the north of Africa and western Asia (Fig. S3) (Nordborg *et al.*, 2005; 1001 Genomes Consortium, 2016).

As dip-inoculation does not distinguish resistance mechanisms based on the leaf surface vs the leaf apoplast, and the lack of disease symptoms could be caused by reduced bacterial multiplication and/or disease tolerance, we further examined the 14 resistant accessions by an infiltration-based infection assay (i.e. by delivering bacterial inoculum directly into the leaf apoplast) and recorded both disease symptoms and bacterial multiplication (Figs 1a,b, S4). The 14 accessions could be categorized into two groups: 12 accessions showed heterogeneous reduction of bacterial growth and disease symptoms, from accessions like Ra-0 showing only a six-fold decrease in bacterial growth (compared to the susceptible Col-0 control) and slightly reduced symptoms, to accessions like Xan-5, in which bacterial growth was reduced more than 650-fold and no symptoms were observed. The other two accessions, Es-0 and Loh-0, were no more resistant to *Pst* DC3000 than Col-0 in an infiltration-based infection assay (Fig. 1a). However, when bacteria were inoculated onto the surface of these two accessions, as was done for the initial screen, it was quite evident that these accessions were resistant to *Pst* DC3000 (Figs 1c, S5).

Accessions showing a hypersensitive-like cell death response to *Pst* DC3000

In an infection using low bacterial inoculum, recognition of effectors by R proteins manifests without any visible symptoms on the plants, as the plant cells that die due to localized programmed cell death are not visible macroscopically. However, when using higher bacterial titers, effector recognition will cause collapse of the infiltrated area by

hypersensitive-like cell death that proceeds much faster (by several hours) than that which is observed due to disease (i.e. the one that would be observed in Col-0 leaves, an accession that does not carry any resistance genes against *Pst* DC3000; Whalen *et al.*, 1991). In order to evaluate if resistance to *Pst* DC3000 in any of the accessions was due to effector recognition (i.e. ETI), accessions were infiltrated with a high bacterial titer of *Pst* DC3000. Six accessions showed a hypersensitive-like cell death response when compared to Col-0, reminiscent of what would be observed for ETI (Table 1; Figs 2a, S6) (Lewis *et al.*, 2010). The hypersensitive-like cell death response was more pronounced for Bu-22, Bu-25, and Xan-5 accessions, with cell death observed for Bu-22 and Bu-25 as early as 18 h post-inoculation. The appearance of cell death in CO and Uk-4 accessions was only slightly faster than in susceptible Col-0 plants, which might reflect why these accessions do not restrict bacterial growth as much as the other 4 accessions (Fig. 1a), as they may mount weaker defense responses.

Several accessions have elevated basal salicylic acid accumulation

Plants that over-accumulate SA have been reported to be more resistant to infection by *Pseudomonas syringae* (Greenberg *et al.*, 1994; Bowling *et al.*, 1997; Jirage *et al.*, 2001; Todesco *et al.*, 2010). We measured SA accumulation in the remaining 6 *Pst* DC3000-resistant accessions that were resistant when bacteria were delivered directly into the apoplast but that did not display a hypersensitive-like cell death response after *Pst* DC3000 inoculation. Three of these accessions had higher accumulation of free and total SA when compared to Col-0 (Fig. 2b), which might explain why these plants were more resistant to *Pst* DC3000 infection, as these high SA concentration levels could potentially prime these accessions for enhanced defense. Under the conditions in which plants were grown, accession Est-1 showed variable accumulation of SA, even though individual plants always had higher SA accumulation than Col-0 plants and this correlated with Est-1 plants always being more resistant to *Pst* DC3000 infection.

In contrast to SA, ABA and JA/JA-Ile accumulation was not significantly different between these *Pst* DC3000-resistant accessions and Col-0 (Fig. S7).

Further characterization of selected resistant accessions with different types of resistance mechanisms

Four out of the 14 *Pst* DC3000-resistant Arabidopsis accessions were chosen for further characterization of their molecular and/or cellular defense responses. Accessions Xan-2 and Xan-5 had a hypersensitive-like cell death response (Table 1), CIBC-16 had an elevated basal accumulation of SA (Fig. 2b), while Ra-0 had a yet-to-be characterized mechanism of resistance. A commonly used marker for the induction of the SA defense pathway is the increase of *PATHOGENESIS-RELATED GENE 1* (*PR1*) transcript and protein accumulation (Yalpani *et al.*, 1991), a response that may be induced by BTH (an SA analogue) (Lawton *et al.*, 1996), but that can also be observed during senescence and after exposure to other stressful environmental stimuli (Sharma *et al.*, 1996; Surplus *et al.*, 1998; Zhang *et al.*, 2013). Consistent with the elevated basal SA accumulation detected in CIBC-16 (Fig. 2b), there was an increased basal accumulation of PR1 protein in this accession (Fig. 3a), whereas no PR1 protein was detectable for Ra-0, an accession whose SA

accumulation was equivalent to that observed for Col-0. Interestingly, Ra-0, Xan-2, and Xan-5 accessions showed higher accumulation of PR1 protein after induction of SA signaling with BTH compared to Col-0 (Fig. 3a).

Recognition of bacteria/PAMPs triggers rapid production of ROS, a phenomenon that is mainly due to bacterial flagellin recognition by the PRR FLS2 (*FLAGELLIN-SENSING 2*) in Arabidopsis (Smith & Heese, 2014). When compared to Col-0, all four resistant accessions showed an increased ROS production after elicitation with *Pst* DC3000 (Fig. 3b). Larger increases were observed for CIBC-16 and Ra-0, compared to Xan-2 and Xan-5, which showed modest ROS increases that were evident in only two out of the three experiments performed.

We also investigated whether the above-mentioned four accessions showed increased resistance to a different pathogenic strain of *Pseudomonas*, *Pseudomonas cannabina* pv. *alisalensis* ES4326R (formerly known as *P. s.* pv. *maculicola* ES4326 or CFBP 1637; Bull *et al.*, 2010) (Figs 4a, S8a). When compared to susceptible Col-0 plants, the four accessions showed increased resistance to *Pcal* ES4326R, with Ra-0 being the least resistant accession of the four, similar to that which was observed for infection with *Pst* DC3000 (Fig. 1a). By contrast, no accession difference was observed for the growth of a non-pathogenic strain, *Pst* DC3000 Δ*hrcC* (in which a structural gene for the T3SS is deleted; Deng & Huang, 1999) (Figs 4b, S8b), suggesting that the mechanisms of resistance are associated with restricting T3SS-dependent growth.

Segregation of the resistance to *Pst* DC3000 in F_2 populations reveals the action of multiple loci

To evaluate the genetic segregation of the resistance to *Pst* DC3000, crosses between 3 resistant accessions, CIBC-16, Ra-0, and Xan-5, to the susceptible accession Col-0 were performed (Fig. S9b–d). The F_2 population of these 3 crosses was inoculated with *Pst* DC3000, and the bacterial numbers within each plant determined (Fig. S10). F_2 individuals were characterized as resistant if their *in planta* bacterial growth was lower than the highest data point for the resistant parent, and susceptible if their bacterial growth was higher than the lowest data point for Col-0. The F_2 segregation of the resistance did not follow a Mendelian segregation that would be expected from the effect of 1 or 2 genes (Fig. 5b–d; Table S4), and many of the F_2 individuals could neither be classified as resistant or susceptible (i.e. their values were above the highest data point for the resistant parent and below the lowest data point for Col-0). Nevertheless, we attempted to map the loci involved in the resistance of these accessions using bulked segregant analysis (BSA) and NGS. Since we expected major genes to be controlling the resistance, we used a method that identifies qualitative traits for mapping (SHOREmap; Sun & Schneeberger, 2015). Unfortunately, no association was observed for any chromosomal region in the F_2 populations for any of the three accessions, suggesting a complicated polygenic nature of the resistance (Fig. S11). This quantitative nature has been observed before in Arabidopsis for resistance to *P. syringae* (Forsyth *et al.*, 2010). The inability to map the loci controlling the resistance after BSA suggests that several gene combinations in the F_2 individuals could create the same resistance phenotype as the one observed in the parents.

Search for bacterial effectors responsible for the hypersensitive cell death response in Xan-5, Bu-22, and Bu-25 accessions

To further investigate whether the hypersensitive-like cell death response in the resistant accessions (Table 1) is due to effector perception by R proteins (i.e. ETI), we inoculated these accessions with *Pst* DC3000 mutant strains in which various effector genes were deleted in order to uncover the relevant effectors responsible for triggering the ETI-type resistance. The three accessions with the fastest cell death response, Bu-22, Bu-25, and Xan-5, were chosen for this analysis. *Pst* DC3000 is reported to contain 36 effector genes (Wei *et al.*, 2015 and Table S5; two identical genes coding for HopAM1 are present in *Pst* DC3000 and counted only once), and a *Pst* DC3000 mutant strain in which 28 of these 36 effector genes are deleted (*Pst Δ28E*; Cunnac *et al.*, 2011) is available. *Pst Δ28E* was unable to cause any visible changes when inoculated into the leaves of any of the resistant accessions (Table S6a), suggesting that one or more of the missing 28 effectors is responsible for the observed hypersensitive-like cell death response.

To identify the specific effectors that cause hypersensitive-like cell death in Bu-22, Bu-25, and Xan-5, we tested other *Pst* DC3000 mutant strains in which smaller subsets of effector genes were deleted. For example, 19 effector genes of *Pst* DC3000 are clustered in the genome and mutant strains deleted in these gene clusters are available (Kvitko *et al.*, 2009; Table S1). However, we found that none of the 19 clustered effectors were responsible for the hypersensitive-like cell death phenotype in Bu-22, Bu-25, or Xan-5 (Table S6b; based on infection with *Pst ΔIΔIIΔIVΔIXΔX*, which has 15 effector genes deleted, and *Pst ΔCEL*, which has 4 effectors deleted). We then inoculated these 3 accessions with a strain with the *avrPto* and *avrPtoB* (*hopAB2*) effector genes deleted. We found that the hypersensitive-like cell death phenotype in Bu-25 was reduced (Table S6c), suggesting that one of these two effectors might be responsible for the resistance to *Pst* DC3000 observed in Bu-25.

To test the potential recognition of the remaining *Pst* DC3000 effectors, we introduced individually each of these eight-effector genes into *Pst Δ28E* and tested if these strains caused any observable changes in the leaves after infiltration. As a positive control, we used a *Pst Δ28E* strain expressing a heterologous effector not present in *Pst* DC3000, *avrRpt2* (which is recognized by the RPS2 resistance protein in Col-0 and therefore capable of causing tissue collapse; Bent *et al.*, 1994) (Fig. 6a). Of the eight strains, only the *Pst Δ28E* strain expressing effector *hopAM1* was capable of causing chlorosis on the leaves of Xan-5 (sometimes, a few chlorotic spots were observed in the other accessions), indicating that this effector could be involved in the resistance phenotype observed for Xan-5 (Table S7; Fig. 6a).

In planta bacterial multiplication confirms the involvement of AvrPto and HopAM1 recognition in resistance to *Pst* DC3000 in Bu-22, Bu-25, Xan-2, and Xan-5 accessions

As the presence of *hopAM1* in *Pst Δ28E* caused a chlorotic response in Xan-5 leaves, we decided to delete this gene from *Pst* DC3000. The *hopAM1* gene is present in 2 duplicated copies in *Pst* DC3000, one on the chromosome (*hopAM1-1*) and the other on the endogenous plasmid A (*hopAM1-2*, formerly known as $avrPpiB2_{Pto}$; Buell *et al.*, 2003). We used strain *Pst* DC3001, which has a 10-kb deletion that includes *hopAM1-2* (Landgraf *et*

al., 2006), to delete *hopAM1-1*. This strain, which was lacking both *hopAM1* genes, was inoculated into Xan-5 at 10^6 CFU ml^{-1} (a titer normally used for disease assays). When compared to *Pst* DC3000, a reproducible increase (4- to 10-fold) in bacterial growth was observed in Xan-5 (Fig. 6b). Because another accession with a hypersensitive-like response, Xan-2, was originally collected in the same region of Azerbaijan as Xan-5, infection of Xan-2 with a strain lacking *hopAM1* was performed. A similar increase in *Pst ΔhopAM1-1ΔhopAM1-2* population compared to *Pst* DC3000 was observed in Xan-2 as had been previously identified for Xan-5 (Fig. S12), suggesting analogous recognition mechanisms for HopAM1 on both Xan-2 and Xan-5. However, deletion of both *hopAM1* genes in *Pst* DC3000 did not fully restore virulence in Xan-2 or Xan-5, as evidenced by the lower final bacterial population when compared to that achieved in Col-0. Furthermore, the resistance of Xan-5 to a strain lacking *hopAM1* was similar to that observed with a strain expressing *avrPphB*, an effector recognized in Col-0 by the resistance protein RPS5 (Warren *et al.*, 1998; Fig. 6b). Therefore, there are more factors besides HopAM1 recognition that influence resistance to *Pst* DC3000 in the Xan-2 and Xan-5 accessions.

Next, we conducted bacterial multiplication assays to determine if the slower cell death response to inoculation by a strain lacking both *avrPto* and *avrPtoB* in Bu-25 (Table S6c) was accompanied by a loss of resistance in this accession. In contrast to *Pst ΔhopAM1-1ΔhopAM1-2* infection of Xan-5, in which only a modest increase in growth was observed when compared to *Pst* DC3000 infection of Xan-5, *Pst ΔavrPtoΔavrPtoB* became fully virulent in Bu-25 (Fig. S13). We also infected Bu-22 and Xan-5 with *Pst ΔavrPtoΔavrPtoB* and found that, remarkably, Bu-22 was also fully susceptible to a strain lacking both effector genes, while Xan-5 maintained full resistance (Fig. S13). The minor (non-statistically significant) increase in growth of *Pst ΔavrPtoΔavrPtoB* observed in Bu-22 in comparison to Col-0 (also notice Fig. 7a for *Pst ΔavrPto* growth in these accessions) might explain why no effect was initially noticed in Bu-22 when evaluating the hypersensitive-like cell death caused by a strain lacking both effector genes, since an increased bacterial growth at earlier infection times could have caused disease-associated cell death to progress faster in Bu-22 than in Col-0.

To evaluate if AvrPto alone, AvrPtoB alone, or both effectors were recognized in Bu-22 and Bu-25, bacterial strains with *avrPto* or *avrPtoB* genes individually deleted were inoculated into plants. No differences in bacterial growth were observed in Bu-22 or Bu-25 after inoculation with either *Pst ΔavrPtoB* or *Pst* DC3000, while a large increase of bacterial growth and the appearance of disease symptoms similar to those observed for *Pst* DC3000 in Col-0 were observed in Bu-22 and Bu-25 accessions inoculated with a strain lacking *avrPto* (Fig. 7a,b). Compared to Bu-22, Bu-25 had a slightly lower bacterial growth when infected with *Pst ΔavrPto*, suggesting that either *Pst ΔavrPto* is more virulent in Bu-22 due to the combined action of *Pst* DC3000 effectors (without AvrPto) or that there is a minor locus in Bu-25 controlling resistance against *Pst* DC3000. Evaluation of the F_2 segregation of the resistance to *Pst* DC3000 in Bu-22 revealed that most likely a single locus controlled recognition of the AvrPto effector (Figs 5a, S9a; Table S4). Bu-25 was collected from the same region in Germany; it remains to be determined whether or not AvrPto recognition in this accession is similar to that of Bu-22. Either way, it seems that AvrPto recognition is the main determinant for resistance to *Pst* DC3000 in both Bu-22 and Bu-25 accessions.

Discussion

We have performed a large-scale screen of 1,041 *A. thaliana* natural accessions to address a fundamental question in plant–pathogen interactions: How many types of resistance mechanisms a plant species may already have against potential infection by a bacterial pathogen that has not apparently co-evolved with the plant species? It is well known that disease phenotypes are strongly influenced by environmental conditions. To select for robustly resistant accessions, we performed our screen under high humidity that simulates disease-conducive conditions (Xin *et al.*, 2016). Of the 14 *Pst* DC3000-resistant accessions identified in this screen, two accessions, Est-1 and Ra-0, had already been shown in previous studies to be more resistant to *Pst* DC3000 infection (Todesco *et al.*, 2010; Hossain & Sultana, 2015), further validating the results of our screen. Other accessions that had been observed before to be resistant to *Pst* DC3000 (Kover & Schaal, 2002; Perchepied *et al.*, 2006; Hossain & Sultana, 2015) were not resistant in our screen, most likely because our disease-conducive (*e.g.*, high humidity) conditions favor the development of disease; therefore, we only characterized accessions with a robust resistance phenotype. Further characterization of the 14 resistant accessions enabled us to classify them into four distinct categories: two accessions had a plant surface-based resistance mechanism, six accessions showed an ETI-like response, three accessions exhibited increased basal SA accumulation, while in the three remaining accessions the mechanism of resistance could not be classified (Fig. S14; Table S8). The mechanisms controlling resistance in these unclassified accessions remain to be determined and could be due to preformed antimicrobial physical barriers or compounds, and/or resistance to bacterial retrieval of nutrients and water during infection. Overall, to our knowledge, this is the first time all four types (possibly more) of pre-existing resistance mechanisms have been uncovered in different individuals of a single host population/species against the same potential pathogen in a single study.

Accessions Es-0 and Loh-0 showed *Pst* resistance only by surface inoculation (Fig. 1c) and do not have a mechanism that restricts *Pseudomonas* growth once the bacteria reach the apoplast. This is interesting because a previous genetic screen identified two Arabidopsis mutants (*scord5* and *scord7*, in the Col-7 genetic background) that were exclusively more susceptible by surface inoculation (but not apoplastic infiltration inoculation) to a coronatine-deficient strain of *Pst* DC3000 (Zeng *et al.*, 2011). Stomata are the most common entry point for foliar infecting Pseudomonads (Melotto *et al.*, 2006), and while the wild-type Col-0 stomata close in response to the coronatine-deficient strain of *Pst* DC3000 as an early defense response in plants, the *scord5* and *scord7* mutant stomata are unable to close after bacterial inoculation. It remains to be determined whether Es-0 and Loh-0 represent natural accessions that have enhanced stomatal defense against *Pst* DC3000. Alternatively, the increased resistance could be caused by a more hostile epiphytic environment experienced by *Pst* DC3000 in these accessions, which would decrease the number of bacteria before they could enter the leaves through the stomata and reach the apoplast. Of note, epiphytic community differences between Arabidopsis accessions have been observed (Horton *et al.*, 2014), so genetic differences among accessions could have an impact on the initial pathogen epiphytic colonization.

Arabidopsis accessions Belm-12, CIBC-16, and Est-1 showed an enhanced basal SA accumulation (Fig. 2b). In Est-1, this elevated SA accumulation is caused by a hyperactive allele of *ACD6* (Rate *et al.*, 1999; Todesco *et al.*, 2010). The loci controlling the *Pst* DC3000 resistance in Belm-12 and CIBC-16 accessions await discovery. Mutagenesis experiments, done mostly in accessions Col-0 and Ler, show that mutant alleles of many Arabidopsis genes cause enhanced SA and *Pst* resistance, including, to name a few, *CPR5*, involved in nuclear pore trafficking (Bowling *et al.*, 1997; Gu *et al.*, 2016); *CPR30*, coding for an F-box protein (Guo *et al.*, 2009); *DND2* (also known as *CNGC4*), encoding a cyclic nucleotide gated channel (Jurkowski *et al.*, 2004); and *ACD2*, coding for an enzyme involved in chlorophyll breakdown (Greenberg *et al.*, 1994; Mach *et al.*, 2001). Almost invariably, SA-enhancing mutants of Col-0 tend to be dwarf, possibly due to the growth-defense tradeoff (Huot *et al.*, 2014). By contrast, Belm-12 and CIBC-16 do not exhibit any obvious dwarfism. As such, it would be interesting in the future to determine why natural accessions like Belm-12 and CIBC-16 can accumulate a high basal level of SA and have elevated pathogen resistance, but maintain apparently normal growth and development.

In addition to leaf-surface- or elevated SA-based resistance, six accessions have an ETI-like response to *Pst* DC3000 infection, with Bu-22, Bu-25, and Xan-5 showing a strong hypersensitive-like cell death response (Table 1). Our further characterization of these three accessions led to identification of *Pst* DC3000 effectors that trigger ETI in these accessions. Specifically, recognition of HopAM1 partially controlled resistance to *Pst* DC3000 in Xan-2 and Xan-5 accessions. When *hopAM1* was expressed from an effectorless *Pst* DC3000 strain, instead of tissue collapse resulting from coalescing cell death (as was observed for expression of *avrRpt2*; Fig. 6a), only enhanced chlorosis was observed. Therefore, HopAM1 recognition in Xan-2 and Xan-5 seems to be involved in a weak ETI-like response. A quantitative nature of the cell death response after HopAM1 bacterial delivery was recently reported in 98 Arabidopsis accessions (Iakovidis *et al.*, 2016). However, even though deletion of *hopAM1* slightly increased bacterial growth in strong ETI-like accession Bur-0 (an accession evaluated in our screen that, unlike Xan-2 and Xan-5, was susceptible to *Pst* DC3000 infection), no correlation was found between the accelerated cell death response and disease resistance, as the same effect of increased bacterial growth for a strain lacking *hopAM1* was observed after infection of both Col-0 and Bur-0 (Iakovidis *et al.*, 2016). The observed lack of increased growth of *Pst ΔhopAM1-1ΔhopAM1-2* in Col-0 plants in this study (although, a slight, non-statistically significant 2-fold growth increase was observed; Figs 6b, S12a) probably reflects the fact that bacterial populations were much higher in our experiments (*c.* 5×10^5 CFU cm^{-2} in Iakovidis *et al.*, 2016; in comparison to 2×10^7 CFU cm^{-2}; Fig. 6b), and, as such, could have been saturated (this same lack of growth difference in Col-0 was observed in a different previous study; Boch *et al.*, 2002). In addition, accessions Xan-2 and Xan-5 are resistant to *Pcal* ES4326R (Fig. 4a), a strain that does not carry HopAM1. This further suggests that the major mechanism(s) controlling resistance to *Pst* DC3000 in Xan-2 and Xan-5 is likely independent of HopAM1 recognition, consistent with the polygenic nature of resistance in Xan-5 based on our analysis of F_2 populations (Figs 5d, S11c).

We found that AvrPto plays a major role in conditioning *Pst* DC3000 resistance in Bu-22 and Bu-25 accessions. AvrPto recognition was first identified in the Solanaceae as being

conferred by a cytoplasmic kinase, Pto, introgressed from *S. pimpinellifolium* into cultivated tomato (Martin *et al.*, 1993). Pto-mediated resistance absolutely requires a nucleotide-binding site–leucine-rich repeat (NBS-LRR) protein (Prf, encoded in the same locus as *Pto* for resistance; Salmeron *et al.*, 1996). Pto can also recognize the structurally unrelated effector AvrPtoB (Kim *et al.*, 2002). In contrast to Pto, the factor controlling resistance in Arabidopsis accessions Bu-22 and Bu-25 recognizes only AvrPto and not AvrPtoB (Fig. 7). Guided by the Pto-AvrPto and Pto-AvrPtoB structures, *Pto* mutations have been made that abolish interaction with AvrPtoB but maintain AvrPto interaction (Dong *et al.*, 2009). Also, alleles of *Pto* have been found in a wild tomato species (*Solanum chmielewskii*) that are capable of recognizing only AvrPtoB (Kraus *et al.*, 2016). In other Solanaceae, phosphorylation of the C-terminus of AvrPto conditions resistance, a domain not involved in Pto-mediated resistance (Yeam *et al.*, 2010). It will be exciting to discover if the *R* gene in Bu-22 and Bu-25 encodes a kinase like *Pto* or a more typical NBS-LRR like *Prf*, and which AvrPto regions are involved in recognition.

The mechanisms that a plant can potentially employ to defend against and evade microbes are numerous. These include, but are not limited to, ETI (Martin *et al.*, 1993), PTI (Zipfel *et al.*, 2004), SAR (Fu & Dong, 2013), elevated basal SA accumulation (Todesco *et al.*, 2010), production of inhibitors of pathogen cell wall degrading enzymes (Ferrari *et al.*, 2006), RNA silencing (Yang *et al.*, 2004), phytoalexin and phytoanticipin production (Fan *et al.*, 2011), toxin detoxification (Johal & Briggs, 1992), and physical barriers to entry and colonization (Melotto *et al.*, 2006). In this study, enhanced PTI, ETI, SA accumulation and defense, and surface-mediated barriers were among the mechanisms that were identified as contributing to resistance in individuals of natural populations of Arabidopsis. These mechanisms were present even though *Pst* DC3000 is apparently not a native pathogen of Arabidopsis, which emphasizes how plants are able to cope with future pathogen attack even if they lack an adaptive immune system similar to that found in vertebrates. The detection of an ETI-like mechanism in some accessions suggests that these accessions are likely co-evolving with some adapted pathogen(s) in nature, and they recognize effectors that happen to be present in *Pst* DC3000. In this sense, ETI can be a ‘cryptic’ defense strategy against infection by emerging new pathogens that carry the same effectors. In fact, it would be advantageous for plants to recognize conserved effectors that are present in multiple pathogens. For example, a study found that *avrPto* was present in more than half of the evaluated *P. syringae* strains (Baltrus *et al.*, 2011), highlighting how this effector recognition could have evolved in nature as a mechanism against Arabidopsis pathogens other than *Pst* DC3000. Remarkably, even though *Pst* DC3000 is not known to be a natural pathogen of *A. thaliana*, under laboratory conditions with dip-inoculation of a high bacterial titer, the vast majority of *A. thaliana* accessions developed visible disease symptoms. Only 14 accessions (*c.* 1.3% of all accessions) were resistant to *Pst* DC3000. This result suggests that, in nature, a major reason for *Pst* DC3000 not being a natural pathogen of *A. thaliana* is likely because of the high inoculum needed for infection and/or a mismatch of the environmental conditions needed for *Pst* DC3000 infection. The molecular basis for the need of a high inoculum and matching environmental conditions are important topics for future studies; however, plants seem to already possess a myriad of mechanisms to defend against a potential invader.

Supplementary Material

Refer to Web version on PubMed Central for supplementary material.

Acknowledgements

We would like to thank Dr Weiqing Zeng for his help in hormone quantification, Dr A. Daniel Jones for (ABA)-d_6, Dr Paul Staswick for JA-Ile, Dr Doug Schemske for the Belm-12 accession, Dr Roger Innes for providing strain *Pst* DC3001, Diane Dunham and Dr Greg Martin for strain *Pst ΔavrPto*, and Dr Alan Collmer, Dr Hailei Wei and Dr Suma Chakravarthy for providing strain *E. coli* S17-1 pCPP5914 and several *Pst* DC3000 mutant strains. Funding was provided by the Gordon and Betty Moore Foundation (GBMF3037 to S.Y.H.), and the National Institutes of Health (GM109928 to S.Y.H.).

References

1001 Genomes Consortium. 1,135 genomes reveal the global pattern of polymorphism in *Arabidopsis thaliana*. Cell. 2016; 166:481–491. [PubMed: 27293186]

Baltrus DA, Nishimura MT, Romanchuk A, Chang JH, Mukhtar MS, Cherkis K, Roach J, Grant SR, Jones CD, Dangl JL. Dynamic evolution of pathogenicity revealed by sequencing and comparative genomics of 19 *Pseudomonas syringae* isolates. PLoS Pathogens. 2011; 7:e1002132. [PubMed: 21799664]

Bent AF, Kunkel BN, Dahlbeck D, Brown KL, Schmidt R, Giraudat J, Leung J, Staskawicz BJ. RPS2 of *Arabidopsis thaliana*: a leucine-rich repeat class of plant disease resistance genes. Science. 1994; 265:1856–1860. [PubMed: 8091210]

Bowling SA, Clarke JD, Liu Y, Klessig DF, Dong X. The *cpr5* mutant of Arabidopsis expresses both NPR1-dependent and NPR1-independent resistance. The Plant Cell. 1997; 9:1573–1584. [PubMed: 9338960]

Buell CR, Joardar V, Lindeberg M, Selengut J, Paulsen IT, Gwinn ML, Dodson RJ, Deboy RT, Durkin AS, Kolonay JF, et al. The complete genome sequence of the Arabidopsis and tomato pathogen *Pseudomonas syringae* pv. *tomato* DC3000. Proceedings of the National Academy of Sciences, USA. 2003; 100:10181–10186.

Boch J, Joardar V, Gao L, Robertson TL, Lim M, Kunkel BN. Identification of *Pseudomonas syringae* pv. *tomato* genes induced during infection of *Arabidopsis thaliana*. Molecular Microbiology. 2002; 44:73–88. [PubMed: 11967070]

Bull CT, Manceau C, Lydon J, Kong H, Vinatzer BA, Fischer-Le Saux M. *Pseudomonas cannabina* pv. *cannabina* pv. nov., and *Pseudomonas cannabina* pv. *alisalensis* (Cintas Koike and Bull, 2000) comb. nov., are members of the emended species *Pseudomonas cannabina* (ex Sutic & Dowson 1959) Gardan, Shafik, Belouin, Brosch, Grimont & Grimont 1999. Systematic and Applied Microbiology. 2010; 33:105–115. [PubMed: 20227217]

Cheng W, Munkvold KR, Gao H, Mathieu J, Schwizer S, Wang S, Yan YB, Wang J, Martin GB, Chai J. Structural analysis of *Pseudomonas syringae* AvrPtoB bound to host BAK1 reveals two similar kinase-interacting domains in a type III Effector. Cell Host & Microbe. 2011; 10:616–626. [PubMed: 22169508]

Choi KH, Kumar A, Schweizer HP. A 10-min method for preparation of highly electrocompetent *Pseudomonas aeruginosa* cells: application for DNA fragment transfer between chromosomes and plasmid transformation. Journal of Microbiological Methods. 2006; 64:391–397. [PubMed: 15987659]

Cunnac S, Chakravarthy S, Kvitko BH, Russell AB, Martin GB, Collmer A. Genetic disassembly and combinatorial reassembly identify a minimal functional repertoire of type III effectors in *Pseudomonas syringae*. Proceedings of the National Academy of Sciences, USA. 2011; 108:2975–2980.

Cuppels DA. Generation and characterization of Tn5 insertion mutations in *Pseudomonas syringae* pv. *tomato*. Applied and Environmental Microbiology. 1986; 51:323–327. [PubMed: 16346988]

Deng WL, Huang HC. Cellular locations of *Pseudomonas syringae* pv. *syringae* HrcC and HrcJ proteins, required for harpin secretion via the type III pathway. Journal of Bacteriology. 1999; 181:2298–2301. [PubMed: 10094714]

Dong J, Xiao F, Fan F, Gu L, Cang H, Martin GB, Chai J. Crystal structure of the complex between *Pseudomonas* effector AvrPtoB and the tomato Pto kinase reveals both a shared and a unique interface compared with AvrPto-Pto. The Plant Cell. 2009; 21:1846–1859. [PubMed: 19509331]

Fan J, Crooks C, Creissen G, Hill L, Fairhurst S, Doerner P, Lamb C. Pseudomonas sax genes overcome aliphatic isothiocyanate-mediated non-host resistance in Arabidopsis. Science. 2011; 331:1185–1188. [PubMed: 21385714]

Ferrari S, Galletti R, Vairo D, Cervone F, De Lorenzo G. Antisense expression of the *Arabidopsis thaliana AtPGIP1* gene reduces polygalacturonase-inhibiting protein accumulation and enhances susceptibility to *Botrytis cinerea*. Molecular Plant–Microbe Interactions. 2006; 19:931–936. [PubMed: 16903359]

Forsyth A, Mansfield JW, Grabov N, de Torres M, Sinapidou E, Grant MR. Genetic dissection of basal resistance to *Pseudomonas syringae* pv. *phaseolicola* in accessions of Arabidopsis. Molecular Plant–Microbe Interactions. 2010; 23:1545–1552. [PubMed: 20653411]

Fu ZQ, Dong X. Systemic acquired resistance: turning local infection into global defense. Annual Review of Plant Biology. 2013; 64:839–863.

Gassmann W, Hinsch ME, Staskawicz BJ. The Arabidopsis RPS4 bacterial-resistance gene is a member of the TIR-NBS-LRR family of disease-resistance genes. The Plant Journal. 1999; 20:265–277. [PubMed: 10571887]

Glaszmann JC, Kilian B, Upadhyaya HD, Varshney RK. Accessing genetic diversity for crop improvement. Current Opinion in Plant Biology. 2010; 13:167–173. [PubMed: 20167531]

Grant MR, Godiard L, Straube E, Ashfield T, Lewald J, Sattler A, Innes RW, Dangl JL. Structure of the Arabidopsis RPM1 gene enabling dual specificity disease resistance. Science. 1995; 269:843–846. [PubMed: 7638602]

Greenberg JT, Guo A, Klessig DF, Ausubel FM. Programmed cell death in plants: a pathogen-triggered response activated coordinately with multiple defense functions. Cell. 1994; 77:551–563. [PubMed: 8187175]

Gou M, Su N, Zheng J, Huai J, Wu G, Zhao J, He J, Tang D, Yang S, Wang G. An F-box gene, *CPR30*, functions as a negative regulator of the defense response in Arabidopsis. The Plant Journal. 2009; 60:757–770. [PubMed: 19682297]

Gu Y, Zebell SG, Liang Z, Wang S, Kang BH, Dong X. Nuclear pore permeabilization is a convergent signaling event in effector-triggered immunity. Cell. 2016; 166:1526–1538. [PubMed: 27569911]

Horton MW, Bodenhausen N, Beilsmith K, Meng D, Muegge BD, Subramanian S, Vetter MM, Vilhjálmsson BJ, Nordborg M, Gordon JI, et al. Genome-wide association study of *Arabidopsis thaliana* leaf microbial community. Nature Communications. 2014; 5:5320.

Hossain MM, Sultana F. Genetic variation for induced and basal resistance against leaf pathogen *Pseudomonas syringae* pv. *tomato* DC3000 among *Arabidopsis thaliana* accessions. SpringerPlus. 2015; 4:296. [PubMed: 26140260]

Huot B, Yao J, Montgomery BL, He SY. Growth-defense tradeoffs in plants: a balancing act to optimize fitness. Molecular Plant. 2014; 7:1267–1287. [PubMed: 24777989]

Iakovidis M, Teixeira PJPL, Exposito-Alonso M, Cowper MG, Law TF, Liu Q, Vu MC, Dang TM, Corwin JA, Weigel D, et al. Effector-triggered immune response in *Arabidopsis thaliana* is a quantitative trait. Genetics. 2016; 204:337–353. [PubMed: 27412712]

Jirage D, Zhou N, Cooper B, Clarke JD, Dong X, Glazebrook J. Constitutive salicylic acid-dependent signaling in *cpr1* and *cpr6* mutants requires PAD4. The Plant Journal. 2001; 26:395–407. [PubMed: 11439127]

Johal GS, Briggs SP. Reductase activity encoded by the HM1 disease resistance gene in maize. Science. 1992; 258:985–987. [PubMed: 1359642]

Jones JD, Dangl JL. The plant immune system. Nature. 2006; 444:323–329. [PubMed: 17108957]

Jurkowski GI, Smith RK Jr, Yu IC, Ham JH, Sharma SB, Klessig DF, Fengler KA, Bent AF. Arabidopsis *DND2*, a second cyclic nucleotide-gated ion channel gene for which mutation causes

the "defense, no death" phenotype. Molecular Plant–Microbe Interactions. 2004; 17:511–520. [PubMed: 15141955]

Kim YJ, Lin NC, Martin GB. Two distinct *Pseudomonas* effector proteins interact with the Pto kinase and activate plant immunity. Cell. 2002; 109:589–598. [PubMed: 12062102]

Kover PX, Schaal BA. Genetic variation for disease resistance and tolerance among *Arabidopsis thaliana* accessions. Proceedings of the National Academy of Sciences, USA. 2002; 99:11270–11274.

Kraus CM, Munkvold KR, Martin GB. Natural variation in tomato reveals differences in the recognition of AvrPto and AvrPtoB effectors from *Pseudomonas syringae*. Molecular Plant. 2016; 9:639–649. [PubMed: 26993968]

Kvitko BH, Collmer A. Construction of *Pseudomonas syringae* pv. *tomato* DC3000 mutant and polymutant strains. Methods in Molecular Biology. 2011; 712:109–128. [PubMed: 21359804]

Kvitko BH, Park DH, Velásquez AC, Wei CF, Russell AB, Martin GB, Schneider DJ, Collmer A. Deletions in the repertoire of *Pseudomonas syringae* pv. *tomato* DC3000 type III secretion effector genes reveal functional overlap among effectors. PLoS Pathogens. 2009; 5:e1000388. [PubMed: 19381254]

Landgraf A, Weingart H, Tsiamis G, Boch J. Different versions of *Pseudomonas syringae* pv. *tomato* DC3000 exist due to the activity of an effector transposon. Molecular Plant Pathology. 2006; 7:355–364. [PubMed: 20507452]

Lawton KA, Friedrich L, Hunt M, Weymann K, Delaney T, Kessmann H, Staub T, Ryals J. Benzothiadiazole induces disease resistance in Arabidopsis by activation of the systemic acquired resistance signal transduction pathway. The Plant Journal. 1996; 10:71–82. [PubMed: 8758979]

Lewis JD, Wu R, Guttman DS, Desveaux D. Allele-specific virulence attenuation of the *Pseudomonas syringae* HopZ1a type III effector via the Arabidopsis ZAR1 resistance protein. PLoS Genetics. 2010; 6:e1000894. [PubMed: 20368970]

Mach JM, Castillo AR, Hoogstraten R, Greenberg JT. The Arabidopsis-accelerated cell death gene *ACD2* encodes red chlorophyll catabolite reductase and suppresses the spread of disease symptoms. Proceedings of the National Academy of Sciences, USA. 2001; 98:771–776.

Malamy J, Carr JP, Klessig DF, Raskin I. Salicylic Acid: a likely endogenous signal in the resistance response of tobacco to viral infection. Science. 1990; 250:1002–1004. [PubMed: 17746925]

Martin GB, Brommonschenkel SH, Chunwongse J, Frary A, Ganal MW, Spivey R, Wu T, Earle ED, Tanksley SD. Map-based cloning of a protein kinase gene conferring disease resistance in tomato. Science. 1993; 262:1432–1436. [PubMed: 7902614]

Melotto M, Underwood W, Koczan J, Nomura K, He SY. Plant stomata function in innate immunity against bacterial invasion. Cell. 2006; 126:969–980. [PubMed: 16959575]

Mur LA, Bi YM, Darby RM, Firek S, Draper J. Compromising early salicylic acid accumulation delays the hypersensitive response and increases viral dispersal during lesion establishment in TMV-infected tobacco. The Plant Journal. 1997; 12:1113–1126. [PubMed: 9418052]

Nordborg M, Hu TT, Ishino Y, Jhaveri J, Toomajian C, Zheng H, Bakker E, Calabrese P, Gladstone J, Goyal R, et al. The pattern of polymorphism in *Arabidopsis thaliana*. PLoS Biology. 2005; 3:e196. [PubMed: 15907155]

Oerke EC. Crop losses to pests. Journal of Agricultural Science. 2006; 144:31–43.

Perchepied L, Kroj T, Tronchet M, Loudet O, Roby D. Natural variation in partial resistance to *Pseudomonas syringae* is controlled by two major QTLs in *Arabidopsis thaliana*. PLoS One. 2006; 1:e123. [PubMed: 17205127]

Rate DN, Cuenca JV, Bowman GR, Guttman DS, Greenberg JT. The gain-of-function Arabidopsis *acd6* mutant reveals novel regulation and function of the salicylic acid signaling pathway in controlling cell death, defenses, and cell growth. The Plant Cell. 1999; 11:1695–1708. [PubMed: 10488236]

Riely BK, Martin GB. Ancient origin of pathogen recognition specificity conferred by the tomato disease resistance gene *Pto*. Proceedings of the National Academy of Sciences, USA. 2001; 98:2059–2064.

Saintenac C, Zhang W, Salcedo A, Rouse MN, Trick HN, Akhunov E, Dubcovsky J. Identification of wheat gene *Sr35* that confers resistance to Ug99 stem rust race group. Science. 2013; 341:783–786. [PubMed: 23811222]

Salmeron JM, Oldroyd GE, Rommens CM, Scofield SR, Kim HS, Lavelle DT, Dahlbeck D, Staskawicz BJ. Tomato *Prf* is a member of the leucine-rich repeat class of plant disease resistance genes and lies embedded within the *Pto* kinase gene cluster. Cell. 1996; 86:123–133. [PubMed: 8689679]

Sharma YK, Léon J, Raskin I, Davis KR. Ozone-induced responses in *Arabidopsis thaliana*: the role of salicylic acid in the accumulation of defense-related transcripts and induced resistance. Proceedings of the National Academy of Sciences, USA. 1996; 93:5099–5104.

Smith JM, Heese A. Rapid bioassay to measure early reactive oxygen species production in Arabidopsis leave tissue in response to living *Pseudomonas syringae*. Plant Methods. 2014; 10:6. [PubMed: 24571722]

Sun H, Schneeberger K. SHOREmap v3.0: fast and accurate identification of causal mutations from forward genetic screens. Methods in Molecular Biology. 2015; 1284:381–395. [PubMed: 25757783]

Surplus SL, Jordan BR, Murphy AM, Carr JP, Thomas B, Mackerness SA. Ultraviolet-B-induced responses in *Arabidopsis thaliana*: role of salicylic acid and reactive oxygen species in the regulation of transcripts encoding photosynthetic and acidic pathogenesis-related proteins. Plant, Cell & Environment. 1998; 21:685–694.

Tateda C, Zhang Z, Shrestha J, Jelenska J, Chinchilla D, Greenberg JT. Salicylic acid regulates Arabidopsis microbial pattern receptor kinase levels and signaling. The Plant Cell. 2014; 26:4171–4187. [PubMed: 25315322]

Thomma BP, Nürnberger T, Joosten MH. Of PAMPs and effectors: the blurred PTI-ETI dichotomy. The Plant Cell. 2011; 23:4–15. [PubMed: 21278123]

Todesco M, Balasubramanian S, Hu TT, Traw MB, Horton M, Epple P, Kuhns C, Sureshkumar S, Schwartz C, Lanz C, et al. Natural allelic variation underlying a major fitness trade-off in *Arabidopsis thaliana*. Nature. 2010; 465:632–636. [PubMed: 20520716]

Tsuda K, Sato M, Glazebrook J, Cohen JD, Katagiri F. Interplay between MAMP-triggered and SA-mediated defense responses. The Plant Journal. 2008; 53:763–775. [PubMed: 18005228]

Tsuda K, Sato M, Stoddard T, Glazebrook J, Katagiri F. Network properties of robust immunity in plants. PLoS Genetics. 2009; 5:e1000772. [PubMed: 20011122]

Wan J, Zhang XC, Neece D, Ramonell KM, Clough S, Kim SY, Stacey MG, Stacey G. A LysM receptor-like kinase plays a critical role in chitin signaling and fungal resistance in Arabidopsis. The Plant Cell. 2008; 20:471–481. [PubMed: 18263776]

Warren RF, Henk A, Mowery P, Holub E, Innes RW. A mutation within the leucine-rich repeat domain of the Arabidopsis disease resistance gene *RPS5* partially suppresses multiple bacterial and downy mildew resistance genes. The Plant Cell. 1998; 10:1439–1452. [PubMed: 9724691]

Wei H-L, Chakravarthy S, Mathieu J, Helmann TC, Stodghill P, Swingle B, Martin GB, Collmer A. *Pseudomonas syringae* pv. *tomato* DC3000 type III secretion effector polymutants reveal an interplay between HopAD1 and AvrPtoB. Cell Host & Microbe. 2015; 17:752–762. [PubMed: 26067603]

Whalen MC, Innes RW, Bent AF, Staskawicz BJ. Identification of *Pseudomonas syringae* pathogens of Arabidopsis and a bacterial locus determining avirulence on both Arabidopsis and soybean. The Plant Cell. 1991; 3:49–59. [PubMed: 1824334]

Yang SJ, Carter SA, Cole AB, Cheng NH, Nelson RS. A natural variant of a host RNA-dependent RNA polymerase is associated with increased susceptibility to viruses by *Nicotiana benthamiana*. Proceedings of the National Academy of Sciences, USA. 2004; 101:6297–6302.

Xiang T, Zong N, Zhang J, Chen J, Chen M, Zhou JM. BAK1 is not a target of the *Pseudomonas syringae* effector AvrPto. Molecular Plant–Microbe Interactions. 2011; 24:100–107. [PubMed: 20923364]

Xin XF, He SY. *Pseudomonas syringae* pv. *tomato* DC3000: a model pathogen for probing disease susceptibility and hormone signaling in plants. Annual Review of Phytopathology. 2013; 51:473–498.

Xin XF, Nomura K, Aung K, Velásquez AC, Yao J, Boutrot F, Chang JH, Zipfel C, He SY. Bacteria establish an aqueous living space as a crucial virulence mechanism. Nature. 2016; 539:524–529. [PubMed: 27882964]

Yalpani N, Silverman P, Wilson TM, Kleier DA, Raskin I. Salicylic acid is a systemic signal and an inducer of pathogenesis-related proteins in virus-infected tobacco. The Plant Cell. 1991; 3:809–818. [PubMed: 1820820]

Yeam I, Nguyen HP, Martin GB. Phosphorylation of the *Pseudomonas syringae* effector AvrPto is required for FLS2/BAK1-independent virulence activity and recognition by tobacco. The Plant Journal. 2010; 61:16–24. [PubMed: 19793077]

Zeng W, Brutus A, Kremer JM, Withers JC, Gao X, Jones AD, He SY. A genetic screen reveals Arabidopsis stomatal and/or apoplastic defenses against *Pseudomonas syringae* pv. *tomato* DC3000. PLoS Pathogens. 2011; 7:e1002291. [PubMed: 21998587]

Zhang K, Halitschke R, Yin C, Liu CJ, Gan SS. Salicylic acid 3-hydroxylase regulates Arabidopsis leaf longevity by mediating salicylic acid catabolism. Proceedings of the National Academy of Sciences, USA. 2013; 110:14807–14812.

Zipfel C, Robatzek S, Navarro L, Oakeley EJ, Jones JD, Felix G, Boller T. Bacterial disease resistance in Arabidopsis through flagellin perception. Nature. 2004; 428:764–767. [PubMed: 15085136]

Summary

- Plants are continuously threatened by pathogen attack, and as such, they have evolved mechanisms to evade, escape, and defend themselves against pathogens. However, it is not known what types of defense mechanisms a plant would already possess to defend against a potential pathogen that has not co-evolved with the plant. We addressed this important question in a comprehensive manner by studying the responses of 1,041 accessions of *Arabidopsis thaliana* to the foliar pathogen *Pseudomonas syringae* pv. *tomato* (*Pst*) DC3000.
- We characterized the interaction using a variety of established methods, including different inoculation techniques, bacterial mutant strains, and assays for the hypersensitive response, salicylic acid (SA) accumulation, and reactive oxygen production.
- Fourteen accessions showed resistance to infection by *Pst* DC3000. Of these, two accessions had a surface-based mechanism of resistance, six accessions showed a hypersensitive-like response, while three had elevated SA levels. Interestingly, *A. thaliana* was discovered to have a recognition system for the effector AvrPto, and HopAM1 was found to modulate *Pst* DC3000 resistance in two accessions.
- Our comprehensive study has significant implications for the understanding of natural disease resistance mechanisms at the species level and for the ecology and evolution of plant–pathogen interactions.

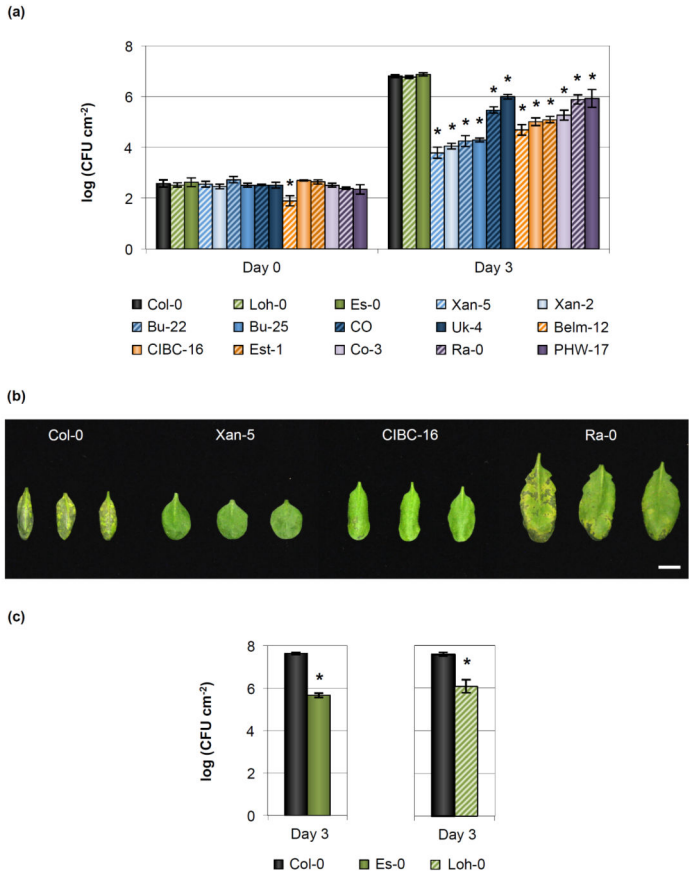

Fig. 1.

Natural variation of resistance to *Pseudomonas syringae* pv. *tomato* (*Pst*) DC3000 amongst Arabidopsis accessions. (a) Bacterial growth in resistant *Arabidopsis thaliana* accessions at 0 and 3 d after syringe-infiltration with 10^5 colony-forming units (CFU) ml^{-1} of *Pst* DC3000. Error bars show ± SE of the mean of 3 (for day 0) or at least 5 (day 3) biological samples. Bars are colored according to the type of resistance observed in this study: green, plant surface-mediated resistance; blue, hypersensitive-like cell death response; orange, enhanced salicylic acid defenses; and purple, unknown. The asterisk indicates accessions whose bacterial growth was significantly different when compared to the susceptible Col-0 control as determined by a Dunnett's test ($P < 0.05$). Statistical analyses for each day after infection were done separately. (b) Disease symptoms in select resistant *A. thaliana* accessions 3 d after syringe-infiltration with 10^5 CFU ml^{-1} of *Pst* DC3000. Bar, 1 cm. Image was composed from accessions' individual images from a single experiment. (c) Bacterial populations are reduced in Es-0 and Loh-0 accessions when bacteria are inoculated on the surface of plants. Bacterial growth was quantified 3 d after dip-inoculation with 10^8 CFU ml^{-1} of *Pst* DC3000. Error bars show ± SE of the mean of 4 biological samples. The asterisk indicates accessions whose bacterial growth was significantly different when compared to the susceptible Col-0 control as determined by a Student's *t*-test ($P < 0.05$).

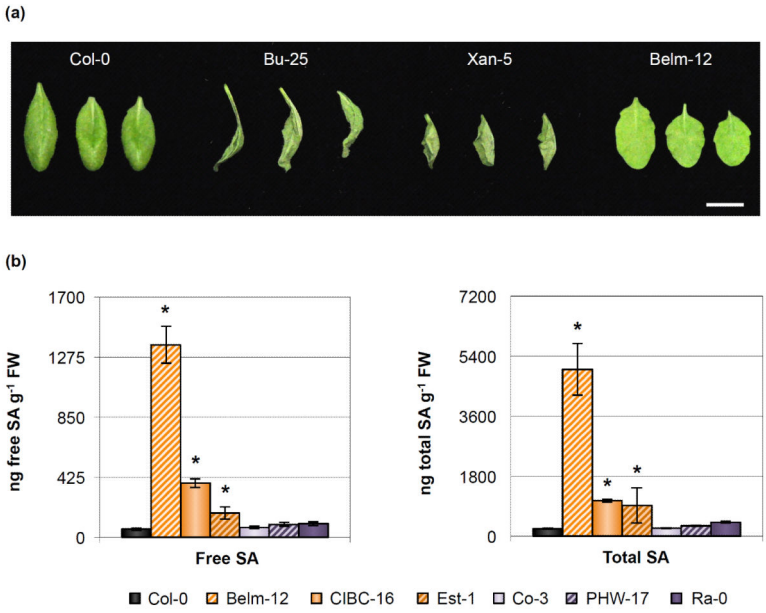

Fig. 2.

Several Arabidopsis accessions either show an accelerated cell death response reminiscent of a hypersensitive response or have higher basal levels of salicylic acid (SA) accumulation. (a) Cell death symptoms 27 h after infiltration with 10^8 colony-forming units (CFU) ml^{-1} of *Pseudomonas syringae* pv. *tomato* (*Pst*) DC3000 in select *Pst* DC3000-resistant ecotypes. Bar, 1 cm. Image was composed from accessions' individual images from a single experiment. (b) Free SA and total SA concentration in 5-wk-old leaves of Col-0 and *Pst* DC3000-resistant accessions. Error bars represent ± SE of the mean from six plants. The asterisk indicates accessions whose hormone concentration was significantly different when compared to the susceptible Col-0 control as determined by a Dunnett's test on the $\log_{10}$-transformed data (so that variances would be homogeneous, $P < 0.05$).

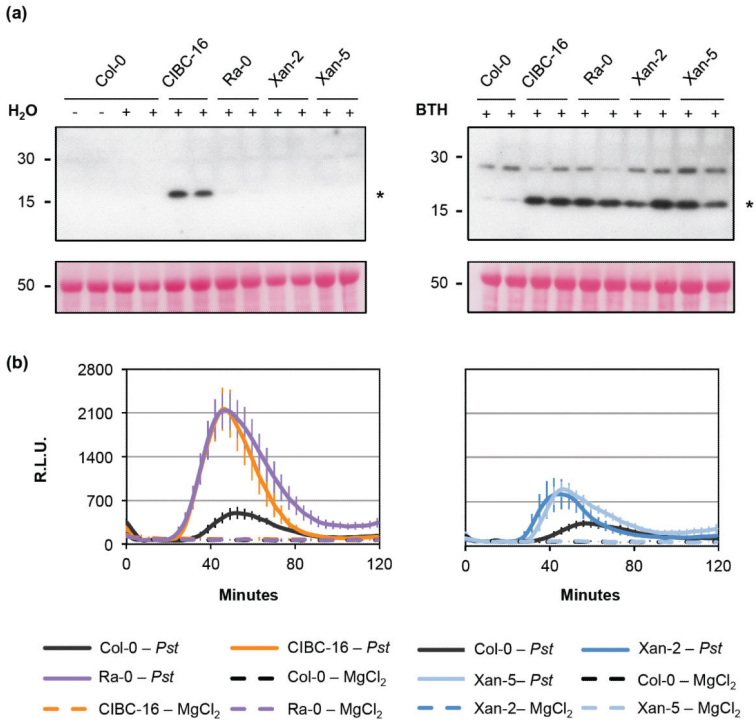

Fig. 3.

Several defense responses are enhanced in *Pseudomonas syringae* pv. tomato (*Pst*) DC3000-resistant Arabidopsis accessions. (a) Pathogenesis-related gene 1 (PR1) protein accumulation 24 h after H_2O and 100 μM benzothiadiazole (BTH) treatment in select *Pst* DC3000-resistant accessions shows an enhanced response after elicitation with BTH. Two samples are shown per each treatment. Untreated (-) Col-0 is shown as a negative control. Proteins were detected using α-PR1 antibodies while the asterisk points to the expected molecular weight of PR1. Bottom image shows the Ponceau S staining of the polyvinylidene difluoride (PVDF) membranes. Twenty μg of total protein were loaded per well. (b) Reactive oxygen species (ROS) production in Col-0 and resistant accessions in response to 2×10^8 colony-forming units (CFU) ml^{-1} *Pst* DC3000 or 0.25 mM $MgCl_2$ as the ROS elicitors. RLU, for relative light units. Error bars show the 95% confidence intervals for the means. Detection was done using SpectraMax L microplate reader (Molecular Devices).

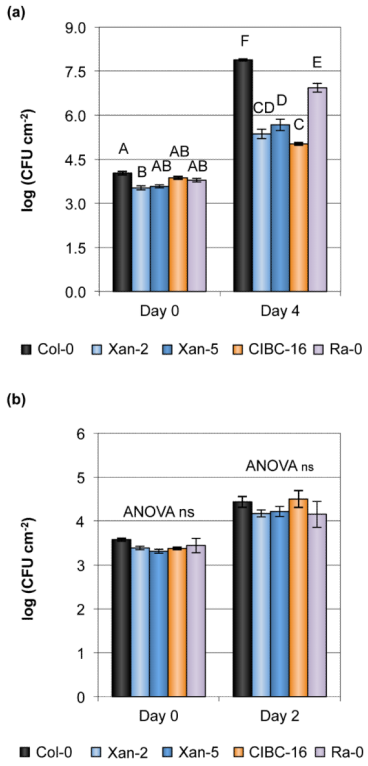

Fig. 4.

Several *Pseudomonas syringae* pv. *tomato* (*Pst*) DC3000-resistant accessions are also resistant to *Pseudomonas cannabina* pv. *alisalensis* (*Pcal*) ES4326R. (a) Bacterial growth in *Arabidopsis thaliana* accessions 0 and 4 d after syringe-infiltration with *Pcal* ES4326R at an inoculum of 5×10^6 colony-forming units (CFU) ml^{-1}. (b) Bacterial growth in *A. thaliana* accessions 0 and 2 d after syringe-infiltration with non-pathogenic *Pst ΔhrcC* at an inoculum of 2×10^6 CFU ml^{-1}. Error bars show ± SE of the mean of 3 (day 0) or at least 5 (days 2 and 4) biological samples. Different letters above the bars indicate significant differences, as determined by a Tukey HSD test ($P < 0.05$). ns, not significant. ANOVA performed separately for each day for (b).

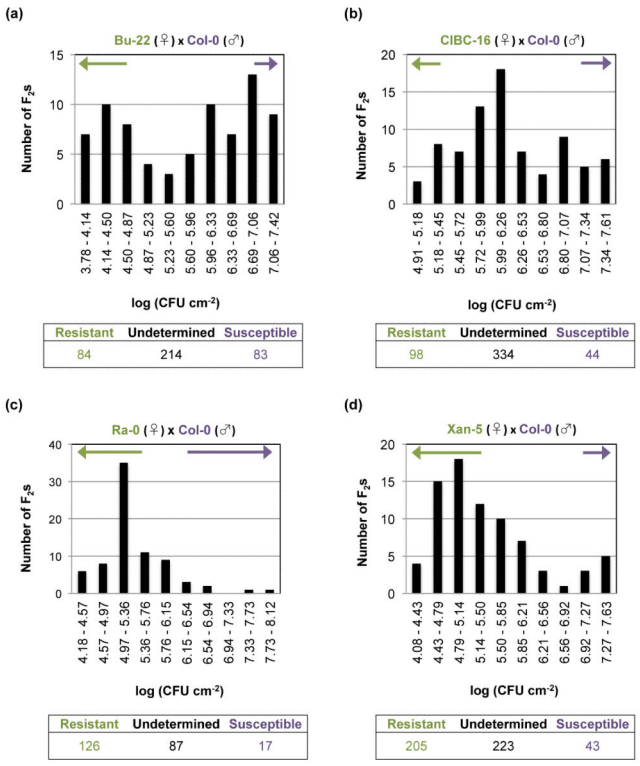

Fig. 5.

Multiple loci are involved in resistance to *Pseudomonas syringae* pv. *tomato* (*Pst*) DC3000 in the resistant Arabidopsis accessions. Segregation of the resistance to *Pst* DC3000 in the F_2 generation derived from crosses of the resistant accessions (♀) (a) Bu-22, (b) CIBC-16, (c) Ra-0, and (d) Xan-5 with the susceptible parent Col-0 (♂). The segregation of the resistance of *c.* 80 individuals is shown in each graph. The arrows above the bars indicate those F_2 individuals that were identified as either resistant (green arrow) or susceptible (purple arrow) to *Pst* DC3000 infection. F_2 individuals were determined as resistant if their value of *in planta* bacterial growth was lower than the highest data point for the resistant parent, and were deemed as susceptible if that value was higher than the lowest data point for the susceptible parent. The table below the graph indicates the segregation of the resistance for all of the F_2 individuals evaluated. CFU, colony-forming units.

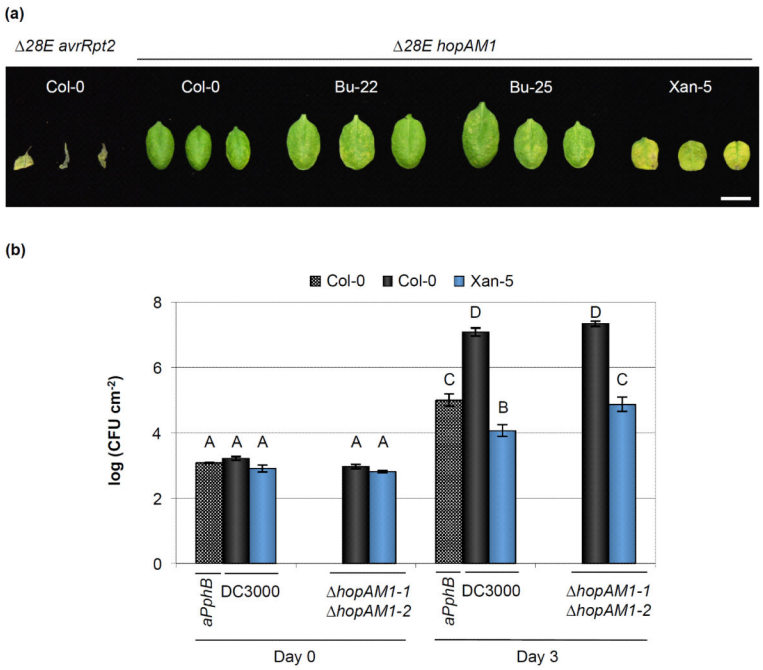

Fig. 6.

HopAM1 recognition influences resistance to *Pseudomonas syringae* pv. *tomato* (*Pst*) DC3000 in the Xan-5 Arabidopsis accession. (a) Cell death symptoms 4 d after inoculation with 2×10^7 colony-forming units (CFU) ml^{-1} of *Pst Δ28E* carrying pBBR:*hopAM1-1* (*Δ28E hopAM1*) and pUCP19::*avrRpt2* (*Δ28 avrRpt2*). Image was composed from accessions' individual images from a single experiment. Bar, 1 cm. *Pst Δ28E avrRpt2* strain was used to confirm that the strain with 28 effectors deleted was still capable of mounting a hypersensitive response (HR) response in Col-0. (b) HopAM1 recognition is partially responsible for the *Pst* DC3000 resistance in the Xan-5 accession. Leaves were infiltrated with *Pst* DC3000, *Pst* DC3001 *ΔhopAM1-1* (*ΔhopAM1-1ΔhopAM1-2*), and *Pst* DC3000 pDSK600::*avrPphB* (*aPphB*) at an inoculum of 10^6 CFU ml^{-1}. Error bars show ± SE of 3 and 6 biological samples for day 0 and day 3, respectively. Letters above each bar indicate similar groups as determined with a Tukey HSD test ($P < 0.05$). A slight reproducible increase in *in planta* bacterial growth was observed for Xan-5 when inoculated with a strain lacking *hopAM1*.

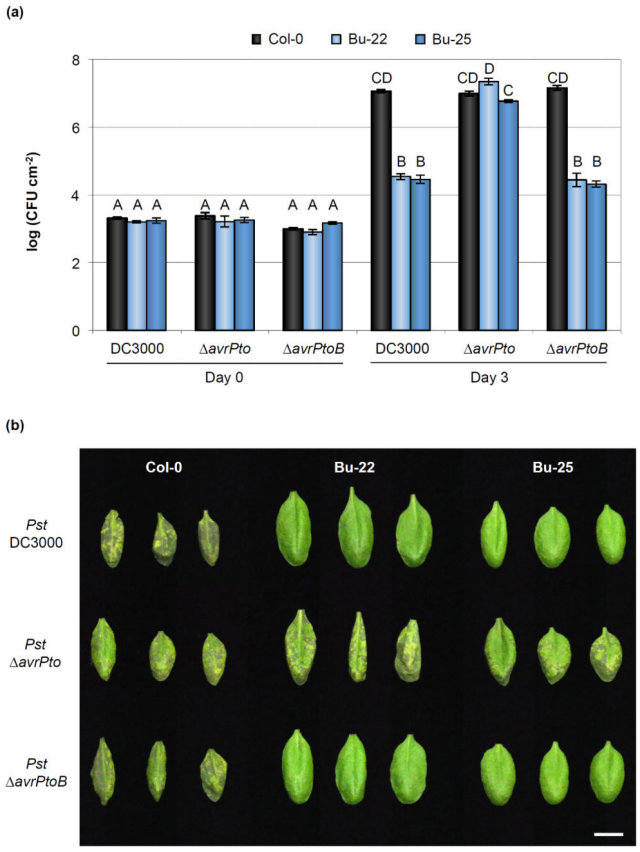

Fig. 7.

AvrPto recognition is a major factor mediating resistance to *Pseudomonas syringae* pv. *tomato* (*Pst*) DC3000 in Bu-22 and Bu-25 Arabidopsis accessions. (a) *In planta* bacterial growth in *Pst* DC3000-resistant accessions after infiltration with *Pst* DC3000, *Pst ΔavrPto*, and *Pst ΔavrPtoB* at an inoculum of 5×10^5 colony-forming units (CFU) ml^{-1}. Error bars show ± SE of 3 and at least 7 biological samples for days 0 and 3, respectively. Letters above each bar indicate similar groups as determined with a Tukey HSD test ($P < 0.05$). Notice that the absence of AvrPto allows *Pst* to multiply to high titers in both Bu-22 and Bu-25 accessions. (b) Disease symptoms 3 d after inoculation with 5×10^5 CFU ml^{-1} of *Pst* DC3000, *Pst ΔavrPto*, and *Pst ΔavrPtoB*. Image was composed from accessions' individual images from a single experiment. Bar, 1 cm.

Table 1

Several Arabidopsis accessions show an accelerated cell death response after being inoculated with high titers of *Pseudomonas syringae* pv. *tomato* (*Pst*) DC3000

Accession	Plant response to *Pst* DC3000 infection			
	No	Partial	Collapsed	Total
Col-0	31	3	2	36
Loh-0	18	0	0	18
Es-0	12	6	0	18
Bu-22	***0***	***5***	***13***	18
Bu-25	***0***	***0***	***24***	24
CO	***13***	***11***	***0***	24
Uk-4	***11***	***11***	***2***	24
Xan-2	***1***	***9***	***8***	18
Xan-5	***0***	***0***	***18***	18
Belm-12	18	0	0	18
CIBC-16	11	7	0	18
Est-1	14	4	0	18
Co-3	17	1	0	18
PHW-17	21	2	1	24
Ra-0	16	2	0	18

Cell death after infiltration with 10^8 colony-forming units (CFU) ml^{-1} *Pst* DC3000 is accelerated in six Arabidopsis accessions, compared to that observed for Col-0. Cell death was evaluated 26 h after infiltration into three categories: (1) no leaf area showing necrosis symptoms; (2) partial necrosis symptoms; (3) fully collapsed leaf. Eighteen to thirty-six leaves were evaluated per accession, with three leaves being infiltrated per plant. Highlighted in bold and in italics are those accessions whose response to *Pst* DC3000 inoculation was different from Col-0, as determined by a Fisher's exact test ($P < 0.0036$).